COMMUNICATIONS IN NUMERICAL METHODS IN ENGINEERING
Commun. Numer. Meth. Engng 2008; **24**:1445–1457
Published online 17 September 2007 in Wiley InterScience (www.interscience.wiley.com). DOI: 10.1002/cnm.1043

Electromechanical analysis of electrostatic nano-actuators using the differential quadrature method

Ming-Hung Hsu*, †

Department of Electrical Engineering, National Penghu University, Penghu, Taiwan

SUMMARY

The nonlinear analysis of nanoelectromechanical systems using the differential quadrature model is investigated. The differential quadrature method is applied to overcome the difficulty of determining the nonlinear equation of motion. The characteristics of various combinations of curved electrodes and cantilever beams are considered to optimize the design. Various nano-actuators, such as the cantilever beam actuator, are derived and simulated to examine the feasibility of applying the differential quadrature method to the nonlinear deflection in solving the nano-actuator problem. The effects of the electrode shapes, the lengths of the actuators, and the moments of inertia of the actuators on the pull-in behavior of the cantilever actuators in electrostatic nanoelectromechanical systems are investigated. The differential quadrature approach is used to generate the electrostatic field equations in matrix form. Copyright © 2007 John Wiley & Sons, Ltd.

Received 27 October 2006; Revised 10 July 2007; Accepted 19 July 2007

KEY WORDS: nanoelectromechanical system; differential quadrature method; nano-actuator; pull-in; electrostatic; nanomechanical behavior

1. INTRODUCTION

Nanotechnology has become a critical technology. The strength of nano-actuators and nanotubes under bending and compression has been modeled and measured experimentally [1–4]. Ke *et al.* [5, 6] studied singly and doubly clamped nanotubes under electrostatic actuation. Keblinski *et al.* [7], Bulashevich and Rotkin [8], and Rotkin *et al.* [9] observed the essentially classical distribution of charge density with a significant charge concentration at the tube end of conductive nanotubes. Beam-type electrostatic actuators that are fabricated from silicon have been widely applied in electromechanical systems. Osterberg and Senturia [10] and Osterberg *et al.* [11]

*Correspondence to: Ming-Hung Hsu, Department of Electrical Engineering, National Penghu University, Penghu, Taiwan.
†E-mail: hsu@npu.edu.tw

presented numerous numerical models to analyze electrostatically deformed diaphragms. They revealed that the electrostatic deformation calculated using the one-dimensional model is close to that obtained using a three-dimensional model. Legtenberg *et al.* [12–14] and Hirai [15–17] studied the dynamic behavior of active joints for various electrostatic actuator designs and the use of a curved electrode to improve the pull-in performance. They applied the Rayleigh–Ritz method to calculate the static deflections of various electrostatic actuators. They also presented the cantilever beam model to elucidate the characteristics of actuators with large displacements, shaped modified electrodes, and cantilevers. Wang [18] applied feedback control to suppress the vibration of an actuator beam in an electrostatic actuator. Shi *et al.* [19] presented a combination of an exterior boundary element method for electrostatics and a finite element method for elasticity to evaluate the effect of coupling between the electrostatic force and the elastic deformation. Hung and Senturia [20] developed leveraged bending and strain-stiffening methods to increase the limiting travel distance before the pull-in of the electrostatic actuators. Chan *et al.* [21] measured the pull-in voltage and capacitance voltage and performed two-dimensional simulations that included the electrical effects of fringing fields and finite beam thickness to determine the material properties of electrostatic actuators. Electrostatic actuators can undergo large deformations at large applied voltages, hence, Li and Aluru [22] developed a mixed-regime approach for combining linear and nonlinear theories. Chyuan *et al.* [23, 24] established the validity and accuracy of the dual boundary element method and studied the effect of gap size variation on the levitation of an electromechanical system. Poncharal *et al.* [25] established that static and dynamic mechanical deflections were electrically induced in cantilevered, multiwalled carbon nanotubes in a transmission electron microscope. They claimed that nanotubes were resonantly excited at the fundamental frequency and higher harmonics as revealed by their deflected contours, which correspond closely to those determined for cantilevered elastic beams. Liew *et al.* [26, 27] examined the elastic and plastic properties of carbon nanotubes under axial tension by performing a molecular dynamics simulation in the microcanonical ensemble.

The increasing availability of various numerical methods, such as the finite difference method, the finite element method, and the boundary element method, has yielded static and dynamic solutions for many complicated structures. However, an alternative more efficient technique for finding these solutions is still sought. This nonlinear equation does not have an analytical solution; however, numerical approaches can help to solve this equation. In seeking an efficient discretization technique to find an accurate numerical solution using a very small number of grid points, the differential quadrature method is utilized to solve numerically the nonlinear partial differential equations. Several nano-actuator designs have been presented to improve the pull-in weakness. The differential quadrature method is employed to formulate the electrostatic field problems in matrix form. The integrity and computational accuracy of the differential quadrature method in solving this problem will be evaluated herein and discussed with reference to a range of case studies. To the best of the author's knowledge, this is the first study to apply the differential quadrature method to nano-actuators.

2. DIFFERENTIAL QUADRATURE METHOD

The differential quadrature method has been widely used to solve a variety of problems in structural mechanics, science, and engineering [28–48]. It has been shown to be a powerful candidate for solving initial and boundary value problems and has thus become a favorable alternative to other

DOI: 10.1002/cnm

methods. Sherbourne and Pandey [28] analyzed the buckling behavior of beams and composite plates using the differential quadrature method. Feng and Bert [29] analyzed the vibration of a geometrically nonlinear beam using the differential quadrature method. Wang *et al.* [30] analyzed the vibration problem of circular annular plates with non-uniform thickness using the differential quadrature method. Kang *et al.* [31] solved the static problem of a curved shaft subjected to end torques using the differential quadrature method. Mirfakhraei and Redekop [32] analyzed the buckling of circular cylindrical shells using the differential quadrature method. Tomasiello [33] analyzed initial boundary value problems using the differential quadrature method. Moradi and Taheri [34] presented a buckling analysis of general laminated composite beams using the differential quadrature method. De Rosa and Franciosi [35] solved dynamic problems of circular arches using the differential quadrature method. Sun and Zhu [36] analyzed incompressible viscous flow problem using the differential quadrature method. Tanaka and Chen [37] presented transient elastodynamic problems using the differential quadrature method. Liew *et al.* [38–45] analyzed structural problems, buckling problems, problems that involved Mindlin plates on winkler foundations, problems that involved thick symmetric cross-ply laminates with first-order shear flexibility, free vibration of rectangular plates with discontinuous edge constraints, fourth-order partial differential equations that governed the bending of thin plates according to classical plate theory, and the axisymmetric free vibration of thick annular plates all using the differential quadrature method. Problems that involve geometric discontinuity cannot be solved using the differential quadrature method. Striz *et al.* [46] undertook a static analysis of structures using the differential quadrature element method. Wang and Gu [47, 48] addressed the static problems of frame structures and free vibration problems of circular plates with stepped thicknesses over a concentric region using the differential quadrature element method. The differential quadrature element method can be used to solve problems with geometric discontinuity. The efficiency and the accuracy of the Galerkin method and the Rayleigh–Ritz method depend on the selected comparison functions. However, the differential quadrature method does not raise this difficulty in selecting the appropriated comparison functions. The core of the differential quadrature method is that the derivative of a function at a particular sample point can be approximated as a weighted linear summation of the values of the function at all of the sample points in the domain. Using this approximation, the differential equation is reduced to a set of algebraic equations. The number of equations depends on the selected number of sample points. For a function $f(z,t)$, the differential quadrature approximation to the mth-order derivative at the ith sampling point is given by

$$\begin{bmatrix} \left.\dfrac{\partial^m f(z,t)}{\partial z^m}\right|_{z=z_1} \\ \left.\dfrac{\partial^m f(z,t)}{\partial z^m}\right|_{z=z_2} \\ \vdots \\ \left.\dfrac{\partial^m f(z,t)}{\partial z^m}\right|_{z=z_N} \end{bmatrix} \cong [D_{ij}^{(m)}] \begin{bmatrix} f(z_1,t) \\ f(z_2,t) \\ \vdots \\ f(z_N,t) \end{bmatrix} \quad \text{for } i,j=1,2,\ldots,N \tag{1}$$

where $f(z_i,t)$ is the value of the function at the sample point z_i and $D_{ij}^{(m)}$ are the weighting coefficients of the mth-order differentiation that is attached to these functional values. The

DOI: 10.1002/cnm

function $f(z,t)$ is

$$f(z,t)=\sum_{i=1}^{N}\frac{M(z)}{(z-z_i)M_1(z_i)}f(z_i,t) \tag{2}$$

where

$$M(z)=\prod_{j=1}^{N}(z-z_j)$$

$$M_1(z_i)=\prod_{j=1,j\neq i}^{N}(z_i-z_j)\quad \text{for } i=1,2,\ldots,N$$

Substituting Equation (2) into Equation (1) yields

$$D_{ij}^{(1)}=\frac{M_1(z_i)}{(z_i-z_j)M_1(z_j)}\quad \text{for } i,j=1,2,\ldots,N \text{ and } i\neq j \tag{3}$$

and

$$D_{ii}^{(1)}=-\sum_{j=1,j\neq i}^{N}D_{ij}^{(1)}\quad \text{for } i=1,2,\ldots,N \tag{4}$$

After the sample points, z_i for $i=1,2,\ldots,N$, have been selected, the coefficients of the weighting matrix can be obtained from Equations (3) and (4). Higher-order derivatives of differential quadrature weighting coefficients can be obtained by matrix multiplication [49]:

$$D_{ij}^{(2)}=\sum_{k=1}^{N}D_{ik}^{(1)}D_{kj}^{(1)}\quad \text{for } i,j=1,2,\ldots,N \tag{5}$$

$$D_{ij}^{(3)}=\sum_{k=1}^{N}D_{ik}^{(1)}D_{kj}^{(2)}\quad \text{for } i,j=1,2,\ldots,N \tag{6}$$

$$D_{ij}^{(4)}=\sum_{k=1}^{N}D_{ik}^{(1)}D_{kj}^{(3)}\quad \text{for } i,j=1,2,\ldots,N \tag{7}$$

The numerical performance of the differential quadrature method depends on the choice of grid point distributions, the type of basis or test functions, geometric features, and boundary conditions. The most convenient approach for solving a beam structure problem is to arrange the sample points uniformly. A non-uniform sample point distribution, such as the Chebyshev–Gauss–Lobatto distribution [49], improves the accuracy of the calculation. The selection of sample points is important for the accuracy of the solution of the differential quadrature method. The unequally spaced Chebyshev–Gauss–Lobatto-distributioned sample points on each beam in this computation satisfy

$$z_i=\frac{L}{2}\left(1-\cos\frac{(i-1)\pi}{N-1}\right)\quad \text{for } i=1,2,\ldots,N \tag{8}$$

DOI: 10.1002/cnm

where L is the length of the beam. The integrity and computational efficiency of the differential quadrature method in solving this problem will be demonstrated using a set of case studies.

3. DEFLECTIONS OF ELECTROSTATIC NANO-ACTUATORS

Figure 1 depicts the geometry of an electrostatic nano-actuator. t_0 specifies the thickness of the cross section of the nano-actuator. The potential energy, U_{vdw}, of the van der Waals attraction is $U_{\text{vdw}} = -C_{\text{h}}A_{\text{s}}/12\pi(d + S - v)^2$ [50, 51], where d is the initial gap, A_{s} is the surface area, C_{h} is the Hamaker constant. The van der Waals force is $q_{\text{vdw}} = -\partial^2 U_{\text{vdw}}/\partial y \partial z$. The shape function S describes the shape of the curved electrode, and is written as a polynomial, $S = \delta_{\max}(z/L)^n$, where $\delta_{\max}$ is the gap between the curved electrode and the nano-beam at $z = L$, n is the polynomial order of electrode shape. The electrode shape varies with n. v is the deflection of the nano-actuator. The potential energy always diverges as the distance $(d + S - v) \to 0$. A minimum separation $(d + S - v)_{\min} \approx 0.2\,\text{nm}$ is commonly assumed in the literature [50, 51]. An electrostatic force, generated by the difference between the voltage applied to the electrode and that applied to the actuator, pulls the cantilever actuator toward the electrode. When the external voltage is applied between the deformable nano-beam and the fixed electrode, a position-dependent electrostatic pressure is generated to pull the deformable beam toward the ground electrode. This electrostatic pressure is approximately proportional to the inverse of the square of the gap between the beam and the electrode. The nano-scale dynamics are approached using continuum physical models. The nano-actuator deflection $v(z, t)$ can be described by the following nonlinear equation:

$$\rho A \frac{\partial^2 v}{\partial t^2} + \frac{\partial^2}{\partial z^2}\left(EI \frac{\partial^2 v}{\partial z^2}\left(1 + \left(\frac{\partial v}{\partial z}\right)^2\right)^{-3/2}\right) = \frac{\varepsilon_0 b_0 V^2}{2(d + S - v)^2}\left(1 + \left(\frac{\partial v}{\partial z}\right)^2\right)^{1/2} + q_{\text{vdw}}\left(1 + \left(\frac{\partial v}{\partial z}\right)^2\right)^{1/2} \tag{9}$$

where E is Young's modulus of the actuator, V is the applied voltage, ε_0 is the permittivity of a vacuum ($\varepsilon_0 = 8.85 \times 10^{-12}\,\text{C}^2\,\text{N}^{-1}\,\text{m}^{-2}$), and b_0 is the width of the actuator. The nano-actuator

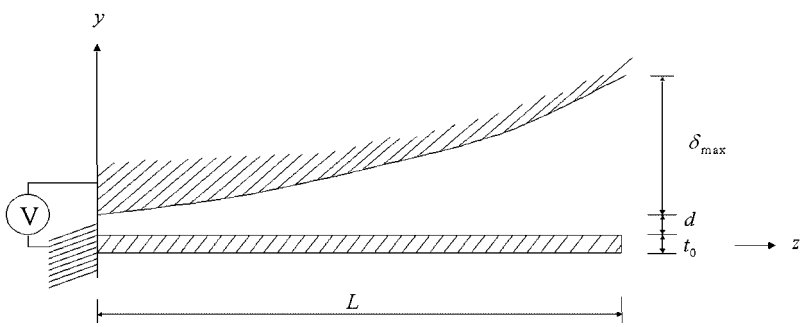

Figure 1. Schematic view of a curved electrode actuator.

DOI: 10.1002/cnm

cross-sectional area is $A = b_0 t_0$. The moment of inertia of the cross-sectional area of the nano-device is $I = b_0 t_0^3/12$. The corresponding boundary conditions of a clamped-free nano-actuator are

$$v(0, t) = 0 \tag{10}$$

$$\frac{\partial v(0, t)}{\partial z} = 0 \tag{11}$$

$$EI\frac{\partial v^2(L, t)}{\partial z^2} = 0 \tag{12}$$

$$\frac{\partial}{\partial z}\left(EI\frac{\partial v^2(L, t)}{\partial z^2}\right) = 0 \tag{13}$$

4. FORMULATION

The differential quadrature method is applied and Equation (1) is substituted into Equation (9). The actuator deflection equation discretizes the sample points as

$$\left[\rho A(z_i)\frac{\partial^2 v}{\partial t^2}\bigg|_{z=z_i}\right]$$

$$+\left[\frac{\partial^2 EI(z)}{\partial z^2}\bigg|_{z=z_i}\left(1+\left(\frac{\partial v}{\partial z}\right)^2\right)^{-3/2}\bigg|_{z=z_i} D_{i1}^{(2)} \quad \frac{\partial^2 EI(z)}{\partial z^2}\bigg|_{z=z_i}\left(1+\left(\frac{\partial v}{\partial z}\right)^2\right)^{-3/2}\bigg|_{z=z_i} D_{i2}^{(2)}\right.$$

$$\left.\cdots \quad \frac{\partial^2 EI(z)}{\partial z^2}\bigg|_{z=z_i}\left(1+\left(\frac{\partial v}{\partial z}\right)^2\right)^{-3/2}\bigg|_{z=z_i} D_{iN}^{(2)}\right][v(z_1, t) \;\; v(z_2, t) \;\; \ldots \;\; v(z_N, t)]^{\mathrm{T}}$$

$$+\left[2\frac{\partial EI(z)}{\partial z}\bigg|_{z=z_i}\left(1+\left(\frac{\partial v}{\partial z}\right)^2\right)^{-3/2}\bigg|_{z=z_i} D_{i1}^{(3)} \quad 2\frac{\partial EI(z)}{\partial z}\bigg|_{z=z_i}\left(1+\left(\frac{\partial v}{\partial z}\right)^2\right)^{-3/2}\bigg|_{z=z_i} D_{i2}^{(3)}\right.$$

$$\left.\cdots \quad 2\frac{\partial EI(z)}{\partial z}\bigg|_{z=z_i}\left(1+\left(\frac{\partial v}{\partial z}\right)^2\right)^{-3/2}\bigg|_{z=z_i} D_{iN}^{(3)}\right][v(z_1, t) \;\; v(z_2, t) \;\; \ldots \;\; v(z_N, t)]^{\mathrm{T}}$$

$$+\left[2\frac{\partial EI(z)}{\partial z}\bigg|_{z=z_i}\frac{\partial}{\partial z}\left(1+\left(\frac{\partial v}{\partial z}\right)^2\right)^{-3/2}\bigg|_{z=z_i} D_{i1}^{(2)} \quad 2\frac{\partial EI(z)}{\partial z}\bigg|_{z=z_i}\right.$$

$$\left.\times \frac{\partial}{\partial z}\left(1+\left(\frac{\partial v}{\partial z}\right)^2\right)^{-3/2}\bigg|_{z=z_i} D_{i2}^{(2)}\right.$$

DOI: 10.1002/cnm

$$\cdots \quad 2\frac{\partial EI(z)}{\partial z}\bigg|_{z=z_i} \frac{\partial}{\partial z}\left(1+\left(\frac{\partial v}{\partial z}\right)^2\right)^{-3/2}\bigg|_{z=z_i} D_{iN}^{(2)}\Bigg][v(z_1,t)\ \ v(z_2,t)\ \ \ldots\ \ v(z_N,t)]^{\mathrm{T}}$$

$$+\left[EI(z_i)\left(1+\left(\frac{\partial v}{\partial z}\right)^2\right)^{-3/2}\bigg|_{z=z_i} D_{i1}^{(4)}\ \ EI(z_i)\left(1+\left(\frac{\partial v}{\partial z}\right)^2\right)^{-3/2}\bigg|_{z=z_i} D_{i2}^{(4)}\right.$$

$$\left.\cdots \quad EI(z_i)\left(1+\left(\frac{\partial v}{\partial z}\right)^2\right)^{-3/2}\bigg|_{z=z_i} D_{iN}^{(4)}\right][v(z_1,t)\ \ v(z_2,t)\ \ \ldots\ \ v(z_N,t)]^{\mathrm{T}}$$

$$+\left[2EI(z_i)\frac{\partial}{\partial z}\left(1+\left(\frac{\partial v}{\partial z}\right)^2\right)^{-3/2}\bigg|_{z=z_i} D_{i1}^{(3)}\ \ 2EI(z_i)\frac{\partial}{\partial z}\left(1+\left(\frac{\partial v}{\partial z}\right)^2\right)^{-3/2}\bigg|_{z=z_i} D_{i2}^{(3)}\right.$$

$$\left.\cdots \quad 2EI(z_i)\frac{\partial}{\partial z}\left(1+\left(\frac{\partial v}{\partial z}\right)^2\right)^{-3/2}\bigg|_{z=z_i} D_{iN}^{(3)}\right][v(z_1,t)\ \ v(z_2,t)\ \ \ldots\ \ v(z_N,t)]^{\mathrm{T}}$$

$$+\left[EI(z_i)\frac{\partial^2}{\partial z^2}\left(1+\left(\frac{\partial v}{\partial z}\right)^2\right)^{-3/2}\bigg|_{z=z_i} D_{i1}^{(2)}\ \ EI(z_i)\frac{\partial^2}{\partial z^2}\left(1+\left(\frac{\partial v}{\partial z}\right)^2\right)^{-3/2}\bigg|_{z=z_i} D_{i2}^{(2)}\right.$$

$$\left.\cdots \quad EI(z_i)\frac{\partial^2}{\partial z^2}\left(1+\left(\frac{\partial v}{\partial z}\right)^2\right)^{-3/2}\bigg|_{z=z_i} D_{iN}^{(2)}\right][v(z_1,t)\ \ v(z_2,t)\ \ \ldots\ \ v(z_N,t)]^{\mathrm{T}}$$

$$=\left[\frac{\varepsilon_0 b_0 V^2}{2(d+S-v)^2}\left(1+\left(\frac{\partial v}{\partial z}\right)^2\right)^{1/2}\bigg|_{z=z_i} + q_{\mathrm{vdw}}\left(1+\left(\frac{\partial v}{\partial z}\right)^2\right)^{1/2}\bigg|_{z=z_i}\right]$$

$$\text{for } i=1,2,\ldots,N \tag{14}$$

Equation (10) can be rewritten as

$$[1\ \ 0\ \ 0\ \ \ldots\ \ 0\ \ 0][v(z_1,t)\ \ v(z_2,t)\ \ v(z_3,t)\ \ \ldots\ \ v(z_{N-1},t)\ \ v(z_N,t)]^{\mathrm{T}}=[0] \tag{15}$$

According to the differential quadrature method, Equation (11) takes the following discrete forms:

$$[D_{1,1}^{(1)}\ \ D_{1,2}^{(1)}\ \ D_{1,3}^{(1)}\ \ \cdots\ \ D_{1,N-1}^{(1)}\ \ D_{1,N}^{(1)}]$$

$$\times[v(z_1,t)\ \ v(z_2,t)\ \ v(z_3,t)\ \ \ldots\ \ v(z_{N-1},t)\ \ v(z_N,t)]^{\mathrm{T}}=[0] \tag{16}$$

DOI: 10.1002/cnm

The boundary conditions at the free end can be rearranged into the following discrete forms:

$$
\begin{aligned}
&[EI(z_N)D^{(2)}_{N,1}\ \ EI(z_N)D^{(2)}_{N,2}\ \ EI(z_N)D^{(2)}_{N,3}\ \ \cdots\ \ EI(z_N)D^{(2)}_{N,N-1}\ \ EI(z_N)D^{(2)}_{N,N}]\\
&\times[v(z_1,t)\ \ v(z_2,t)\ \ v(z_3,t)\ \ \ldots\ \ v(z_{N-1},t)\ \ v(z_N,t)]^{\mathrm{T}}=[0]\\
&\left[\left.\frac{\partial EI(z)}{\partial z}\right|_{z=z_N} D^{(2)}_{N,1}\ \left.\frac{\partial EI(z)}{\partial z}\right|_{z=z_N} D^{(2)}_{N,2}\ \left.\frac{\partial EI(z)}{\partial z}\right|_{z=z_N} D^{(2)}_{N,3}\right.\\
&\left.\cdots\ \left.\frac{\partial EI(z)}{\partial z}\right|_{z=z_N} D^{(2)}_{N,N-1}\ \left.\frac{\partial EI(z)}{\partial z}\right|_{z=z_N} D^{(2)}_{N,N}\right]\\
&\times[v(z_1,t)\ \ v(z_2,t)\ \ v(z_3,t)\ \ \ldots\ \ v(z_{N-1},t)\ \ v(z_N,t)]^{\mathrm{T}}\\
&+[EI(z_N)D^{(3)}_{N,1}\ \ EI(z_N)D^{(3)}_{N,2}\ \ EI(z_N)D^{(3)}_{N,3}\ \ \cdots\ \ EI(z_N)D^{(3)}_{N,N-1}\ \ EI(z_N)D^{(3)}_{N,N}]\\
&\times[v(z_1,t)\ \ v(z_2,t)\ \ v(z_3,t)\ \ \ldots\ \ v(z_{N-1},t)\ \ v(z_N,t)]^{\mathrm{T}}=[0]
\end{aligned}
\tag{17}
$$

Many inner and boundary points in the computational domain contribute directly to the calculation of the derivatives and the state variables themselves due to the global nature of the differential quadrature method.

5. RESULTS AND DISCUSSION

Figure 2 shows the clamped-free actuator frequencies that are solved using finite element and differential quadrature methods. The material and geometric parameters of actuators are $E = 150\,\mathrm{GPa}$, $b_0 = 10\,\mathrm{nm}$, and $t_0 = 10\,\mathrm{nm}$. The finite element method, which can transform differential equations into a set of algebraic equations, assumes the shape of a solution in the element domain and satisfies equilibrium. The Euler–Bernoulli element is utilized in this nano-beam model. The numerical results imply that the actuator frequencies calculated from the differential quadrature method are very consistent with the numerical results that are obtained using the finite element method. The effect of the actuator length becomes more pronounced for higher-mode frequencies. Figure 3 compares the tip deflections at various applied voltages for variously shaped electrodes to elucidate the feasibility of using the differential quadrature method to solve the fixed–free beam-type actuator and the accuracy of the differential quadrature method. The material and geometric parameters of the actuators are [12] $E = 150\,\mathrm{GPa}$, $\delta_{\max} = 30\,000\,\mathrm{nm}$, $b_0 = 5000\,\mathrm{nm}$, $t_0 = 2000\,\mathrm{nm}$, $d = 2000\,\mathrm{nm}$, and $L = 500\,000\,\mathrm{nm}$. Simulated results are compared with experimental results in the literature [12]. The van der Waals interaction is important only when the gap between the nano-device and the fixed electrode is small. It can be neglected in an analysis with large gaps. The results imply that the tip deflections calculated from the differential quadrature method are very consistent with the experimental results in the literature [12] for $n = 2$. The practical electrostatic field between the clamped-free beam and the fixed electrode is not distributed uniformly. A difference between the experimental results [12] and the numerical results is observed for $n = 1$. The difference may arise from ignoring the fringing effect of the electric field at the free end. The effect of the shape of an electrode on the tip deflection in a curved electrode system is investigated using the differential

DOI: 10.1002/cnm

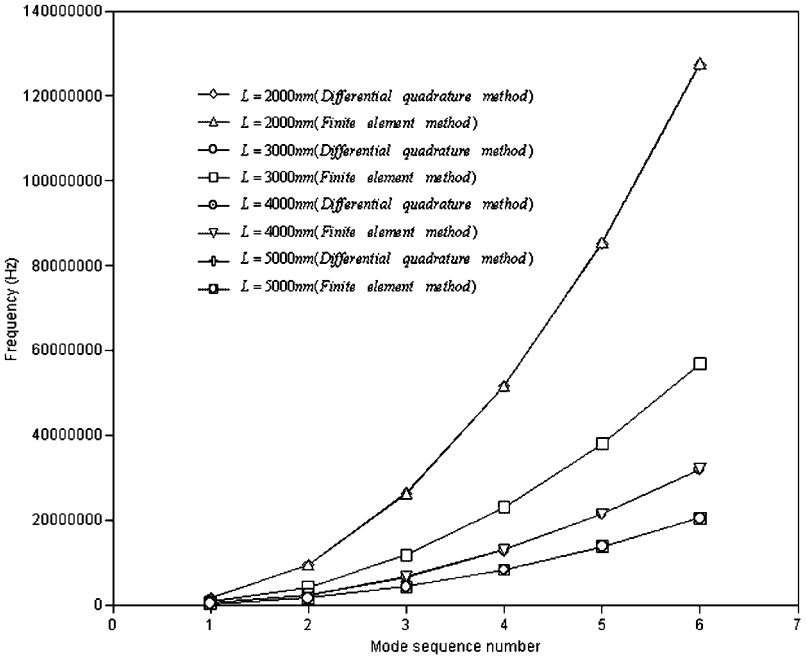

Figure 2. Frequencies of clamped–free nano-actuators.

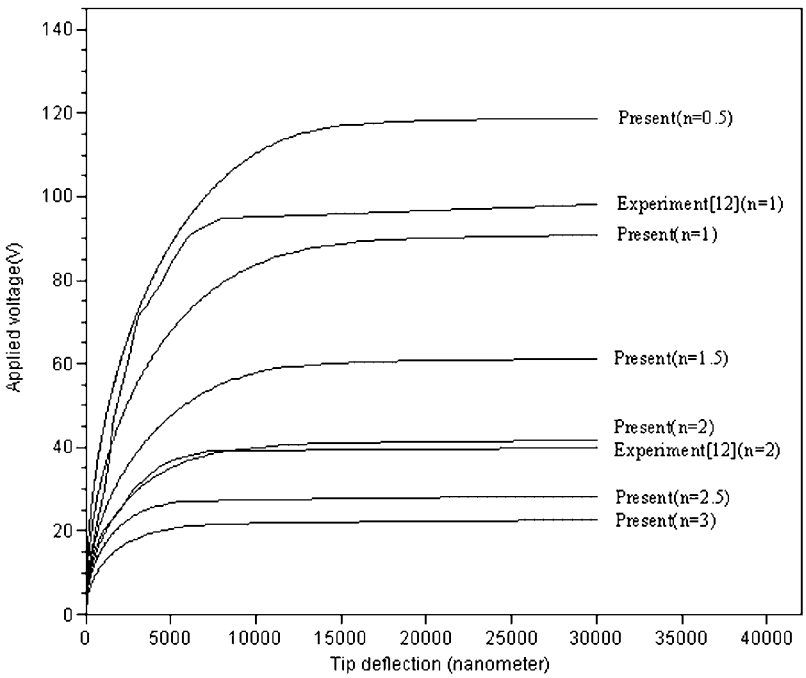

Figure 3. Comparison of tip deflections with various applied voltages and electrode shapes.

DOI: 10.1002/cnm

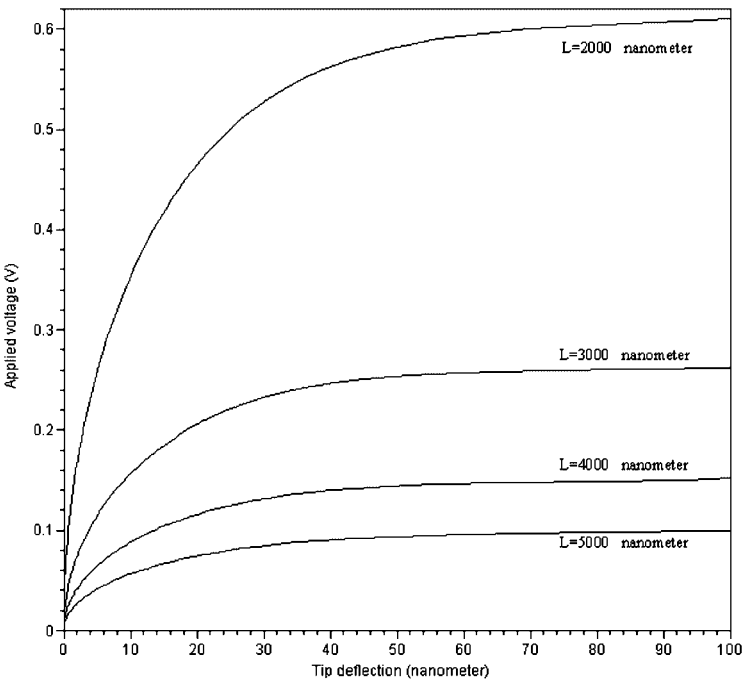

Figure 4. Comparison of tip deflections with different lengths of nano-actuators.

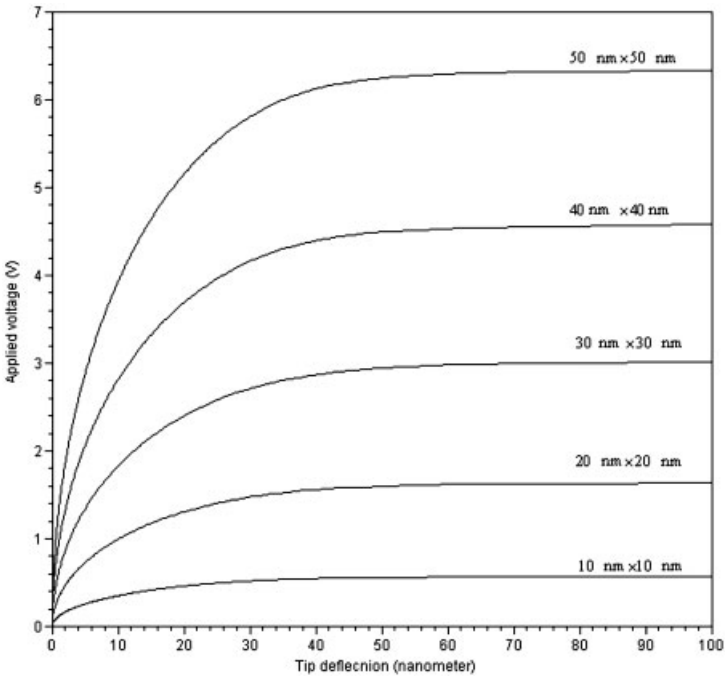

Figure 5. Comparison of tip deflections with varying cross sections of nano-actuators.

DOI: 10.1002/cnm

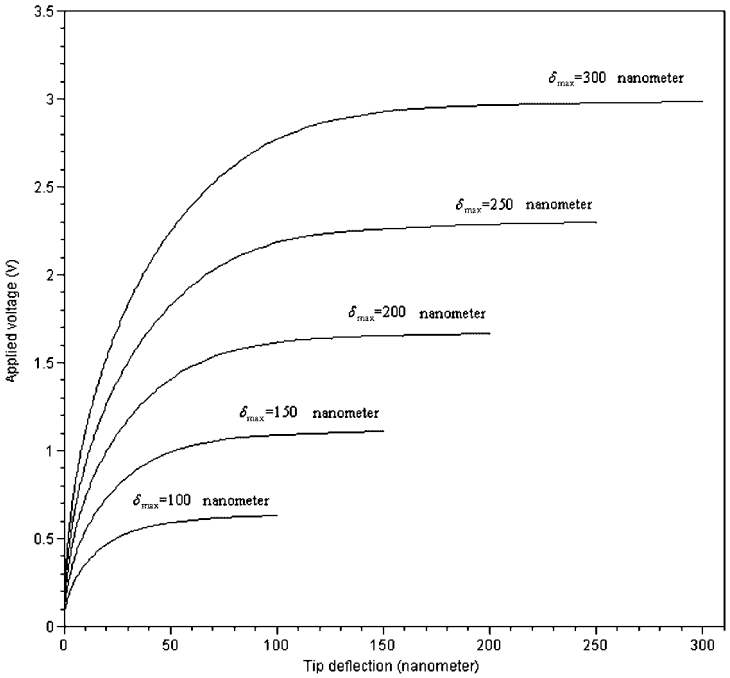

Figure 6. Comparison of tip deflections for different $\delta_{\max}$ values.

quadrature model. Figure 4 plots the tip deflections of the actuators that correspond to different lengths. The material and geometric parameters of the devices are $E = 150\,\text{GPa}$, $\delta_{\max} = 100\,\text{nm}$, $b_0 = 10\,\text{nm}$, and $t_0 = 10\,\text{nm}$. The effects of the lengths of the nano-actuators on the deflections are examined. Numerical results reveal that the stiffness of the nano-actuator increases as the length of the device decreases. The normalized deflections effectively increase with the relative lengths of the nano-actuator. Figure 5 compares the tip deflections with various sections of the nano-actuators. As the moments of inertia of the nano-actuators increase, the normalized deflections effectively decrease. Figure 6 compares the tip deflections for various $\delta_{\max}$. Interestingly, the pull-in voltage more than quadruples as $\delta_{\max}$ changes from 100 to 300 nm.

6. CONCLUSIONS

Numerical results indicate that the differential quadrature method can efficiently provide accurate estimates of pull-in voltage for different electrostatic nano-actuators. The numerical results demonstrate that the actuator frequencies calculated using the differential quadrature method agree closely with the numerical results obtained using the finite element method. The electrode shapes, the lengths of the actuators, and the moments of inertia of the actuators strongly affect the pull-in behavior of the cantilever actuators in electrostatic nanoelectromechanical systems. Changing the shape of an electrode in an electrostatic nano-actuator is an effective method of varying the distribution of electrostatic forces. A more general conclusion of this research is that

DOI: 10.1002/cnm

differential quadrature approach can be used to solve nonlinear partial differential equations. Hence, this methodology may be applied to solve more complicated problems in other fields of science.

REFERENCES

1. Wu DH, Chien WT, Chen CS, Chen HH. Resonant frequency analysis of fixed-free single-walled carbon nanotube-based mass sensor. *Sensors and Actuators A* 2006; **126**:117–121.
2. Yakobson BI, Brabec CJ, Bernholc J. Nanomechanics of carbontubes. *Physical Review Letters* 1996; **76**: 2511–2514.
3. Krishnan A, Dujardin E, Ebbesen TW, Yianilos PN, Treacy MMJ. Young's modulus of single-walled nanotubes. *Physical Review B* 1998; **58**:14–19.
4. Rafii-Tabar H. Computational modeling of thermo-mechanical and transport properties of carbon nanotubes. *Physics Reports* 2004; **390**:235–452.
5. Ke CH, Espinosa HD, Pugno N. Numerical analysis of nanotube based NEMS devices-part II: role of finite kinematics, stretching and charge concentrations. *Journal of Applied Mechanics* 2005; **72**:726–731.
6. Pugno N, Ke CH, Espinosa HD. Analysis of doubly-clamped nanotube devices under large displacements. *Journal of Applied Mechanics* 2005; **72**:445–449.
7. Keblinski P, Nayak SK, Zapol P, Ajayan PM. Charge distribution and stability of charged carbon nanotube. *Physical Review Letter* 2002; **89**:255–503.
8. Bulashevich KA, Rotkin SV. Nanotube device: a micro-scopic model. *JETP Letter* 2002; **175**:205–209.
9. Rotkin SV, Shrivastava V, Bulashevich KA, Aluru NR. Atomic capacitance of a nanotube electrostatic device. *International Journal of Nanoscience* 2002; **1**:337–346.
10. Osterberg PM, Senturia SD. M-test: a test chip for MEMS material property measurement using electrostatically actuated test structures. *Journal of Microelectromechanical Systems* 1997; **6**:107–117.
11. Osterberg PM, Yie H, Cai X, White J, Senturia S. Self-consistent simulation and modeling of electrostatically deformed diaphragms. *Proceedings of IEEE Conference on Micro Electro Mechanical Systems*, Oiso, Japan, 1994; 28–32.
12. Legtenberg R, Gilbert Senturia JSD, Elwenspoek M. Electrostatic curved electrode actuators. *Journal of Microelectromechanical Systems* 1997; **6**:257–265.
13. Elwenspoek M, Weustink M, Legtenberg R. Static and dynamic properties of active joints. *The 8th International Conference on Solid-State Sensors and Actuators*, Stockholm, Sweden, 1995; 412–415.
14. Legtenberg R, Berenschot E, Elwenspoek M, Fluitman J. Electrostatic curved electrode actuators. *Proceedings of IEEE Conference on Micro Electro Mechanical Systems*, Amsterdam, The Netherlands, 1995; 37–42.
15. Hirai Y, Marushima Y, Nishikawa K, Tanaka Y. Young's modulus evaluation of Si thin film fabricated by compatiable process with Si MEMS's. *International Conference on Microprocesses and Nanotechnology*, Tokyo, Japan, 2002; 82–83.
16. Hirai Y, Marushima Y, Soda S. Electrostatic actuator with novel shaped cantilever. *Proceedings of International Symposium on Micromechatronics and Human Science*, U.S.A., 2000; 223–227.
17. Hirai Y, Shindo M, Tanaka Y. Study of large bending and low voltage drive electrostatic actuator with novel shaped cantilever and electrode. *Proceedings of International Symposium on Micromechatronics and Human Science*, Nagoya, Japan, 1998; 161–164.
18. Wang PKC. Feedback control of vibrations in a micromachined cantilever beam with electrostatic actuators. *Journal of Sound and Vibration* 1998; **213**:537–550.
19. Shi F, Ramesh P, Mukherjee S. Simulation methods for micro-electro-mechanical structures (MEMS) with application to a microtweezer. *Computers and Structures* 1995; **56**:769–783.
20. Hung ES, Senturia SD. Extending the travel range of analog-tuned electrostatic actuators. *Journal of Microelectromechanical Systems* 1999; **8**:497–505.
21. Chan EK, Garikipati K, Dutton RW. Characterization of contact electromechanics through capacitance-voltage measurements and simulations. *Journal of Microelectromechanical Systems* 1999; **8**:208–217.
22. Li G, Aluru NR. Linear, nonlinear and mixed-regime analysis of electrostatic MEMS. *Sensors and Actuators* 2001; **91**:278–291.
23. Chyuan SW, Liao YS, Chen JT. An efficient method for solving electrostatic problems. *Computing in Science and Engineering* 2003; **5**:52–58.
24. Chyuan SW, Liao YS, Chen JT. Computational study of variations in gap size for the electrostatic levitating force of MEMS device using dual BEM. *Microelectronics Journal* 2004; **35**:739–748.

DOI: 10.1002/cnm

25. Poncharal P, Wang ZL, Ugarte D, de Heer WA. Electrostatic deflections and electromechanical resonances of carbon nanotubes. *Science* 1999; **283**:1513–1516.
26. Liew KM, He XQ, Wong CH. On the study of elastic and plastic properties of multi-walled carbon nanotubes under axial tension using molecular dynamics simulation. *Acta Materialia* 2004; **52**:2521–2527.
27. Liew KM, Wong CH, He XQ, Tan MJ, Meguid SA. Nanomechanics of single and multiwalled carbon nanotubes. *Physical Review B* 2004; **69**:115429.
28. Sherbourne AN, Pandey MD. Differential quadrature method in the buckling analysis of beams and composite plates. *Computers and Structures* 1991; **40**:903–913.
29. Feng Y, Bert CW. Application of the quadrature method to flexural vibration analysis of a geometrically nonlinear beam. *Nonlinear Dynamics* 1992; **3**:13–18.
30. Wang X, Yang J, Xiao J. On free vibration analysis of circular annular plates with non-uniform thickness by the differential quadrature method. *Journal of Sound and Vibration* 1995; **184**:547–551.
31. Kang K, Bert CW, Striz AG. Static analysis of a curved shaft subjected to end torques. *International Journal of Solids and Structures* 1996; **33**:1587–1596.
32. Mirfakhraei P, Redekop D. Buckling of circular cylindrical shells by the differential quadrature method. *International Journal of Pressure Vessels and Piping* 1998; **75**:347–353.
33. Tomasiello S. Differential quadrature method: application to initial-boundary-value problems. *Journal of Sound and Vibration* 1998; **218**:573–585.
34. Moradi S, Taheri F. Delamination buckling analysis of general laminated composite beams by differential quadrature method. *Composite*, *Part B* 1999; **30**:503–511.
35. De Rosa MA, Franciosi C. Exact and approximate dynamic analysis of circular arches using DQM. *International Journal of Solids and Structures* 2000; **37**:1103–1117.
36. Sun J, Zhu Z. Upwind local differential quadrature method for solving incompressible viscous flow. *Computer Methods in Applied Mechanics and Engineering* 2000; **188**:495–504.
37. Tanaka M, Chen W. Dual reciprocity BEM applied to transient elastodynamic problems with differential quadrature method in time. *Computer Methods in Applied Mechanics and Engineering* 2001; **190**:2331–2347.
38. Liew KM, Han JB, Xiao ZM. Differential quadrature method for thick symmetric cross-ply laminates with first-order shear flexibility. *International Journal of Solids and Structures* 1996; **33**:2647–2658.
39. Du H, Liew KM, Lim MK. Generalized differential quadrature method for buckling analysis. *Journal of Engineering Mechanics* 1996; **122**:95–100.
40. Liew KM, Han JB, Xiao ZM, Du H. Differential quadrature method for mindlin plates on winkler foundations. *International Journal of Mechanical Sciences* 1996; **38**:405–421.
41. Liew KM, Lam KY. Vibration analysis of multi-span plates having orthogonal straight edges. *Journal of Sound and Vibration* 1991; **147**:255–264.
42. Liew KM, Hung KC, Sum YK. Flexural vibration of polygonal plates: treatments of sharp re-entrant corners. *Journal of Sound and Vibration* 1995; **183**:221–238.
43. Lim CW, Liew KM. Vibrations of perforated plates with rounded corners. *Journal of Engineering Mechanics* 1995; **121**:203–213.
44. Liew KM, Liu FL. Differential cubature method: a solution technique for Kirchhoff plates of arbitrary shape. *Computer Methods in Applied Mechanics and Engineering* 1997; **145**:1–10.
45. Han JB, Liew KM. Axisymmetric free vibration of thick annular plates. *International Journal of Mechanical Sciences* 1999; **41**:1089–1109.
46. Striz AG, Chen W, Bert CW. Static analysis of structures by the quadrature element method (QEM). *International Journal of Solids and Structures* 1994; **31**:2807–2818.
47. Wang X, Gu H. Static analysis of frame structures by the differential quadrature element method. *International Journal for Numerical Methods in Engineering* 1997; **40**:759–772.
48. Gu HZ, Wang XW. On the free vibration analysis of circular plates with stepped thickness over a concentric region by the differential quadrature element method. *Journal of Sound and Vibration* 1997; **202**:452–459.
49. Bert CW, Mailk M. Differential quadrature method in computational mechanics: a review. *Applied Mechanics Reviews* 1996; **49**:1–28.
50. Israelachvili JN. *Intermolecular and Surface Forces*. Academic Press: New York, 1992.
51. Drexler KE. *Nanosystems*. Wiley: New York, 1992.

DOI: 10.1002/cnm